Stress Gradient Correction Factor for Stress Intensity at Welded Gusset Plates

Stress gradient correction factor is determined for gusset plates with circular transitions and groove welded to flange tips

BY N. ZETTLEMOYER AND J. W. FISHER

Introduction

The driving force behind fatigue crack propagation is the range of stress intensity factor, ΔK. This parameter is often evaluated by superimposing various correction factors on ΔK for a central, through crack in an infinite plate under uniaxial tension.[1,6,10,12,14,19] One of the correction factors, F_g, is the stress gradient correction factor and is intended to account for either a nonuniform applied stress (such as bending) or stress concentration caused by detail geometry.

The authors[19] evaluated F_g for stiffener and cover plate details. The procedure employed is often called the Green's function or superposition approach.[8,9,12,16,17] In this approach the stresses in the crack free body are used to estimate stress intensity by means of an appropriate Green's function. The advantage is that only one stress analysis (usually made by the finite element technique) needs to be made for each joint geometry. The only requirement is that the crack plane be known in advance.

The objectives of the subject study were:

1. To determine F_g for gusset plates with circular transitions and groove welded to flange tips.
2. To provide for the automatic prediction of F_g for any crack length and arbitrary detail geometry.

In general, the procedure previously described by the authors[19] was followed; the only major difference was the detail involved.

N. ZETTLEMOYER is Research Engineer, Exxon Production Research Co., Houston, Texas; J. W. FISHER is Professor of Civil Engineering, Fritz Engineering Laboratory, Lehigh University, Bethlehem, Pennsylvania.

Crack Free Stress Analysis

Analytical Model

The basic geometry for the gusset plate investigation is shown in Fig. 1. Symmetry was assumed about the gusset midlength and the web centerline. (The implied symmetrical gussets on opposite flange tips are common in bridges and also maximize stress concentration.[7]) Full penetration of the weld was the only case considered; the weld depth was taken as constant and equal to the gusset plate thickness. The termination of the weld at the point of transition tangency was assumed to be ground smooth to maintain the intended contour. The weld thickness in the plane of the flange and gusset was taken as part of the gusset width.

Four variables were studied. They were the transition radius R, the attachment length L, the gusset plate width W_{gp}, and the gusset plate thickness T_{gp}. Table 1 lists the parametric combinations investigated. Each of the variables was nondimensionalized by either flange width or thickness. The flange width was typically 12 in. (305 mm). All problems were analyzed two-dimensionally; hence, only the relative plate thicknesses were important. Eccentricity of the gusset plate's centroidal plane at midthickness relative to the flange centroidal plane was neglected.

Plane stress elements from an existing finite element computer program, SAP IV[3], were used for the stress analysis. Young's modulus was set at 29,600 ksi (2×10^5 MPa), and Poisson's ratio was taken to be 0.30. The fact that a gusset transition was assumed greatly simplified the investigation since no singularity existed at the detail. Thus, the very fine mesh sizes used in the previous stiffener and cover plate analyses[19] were unnecessary. Still, as the radius decreased concentration increased and the emphasis on mesh size also increased. The mesh size had to be small enough in each geometry to capture the peak concentration.

Uniform stress was input to a two-dimensional coarse mesh which employed plane stress elements. For gussets with large transition radii ($R/W_f \geq 0.5$), the element with the highest stress was located and that value was used to determine the maximum stress concentration factor,

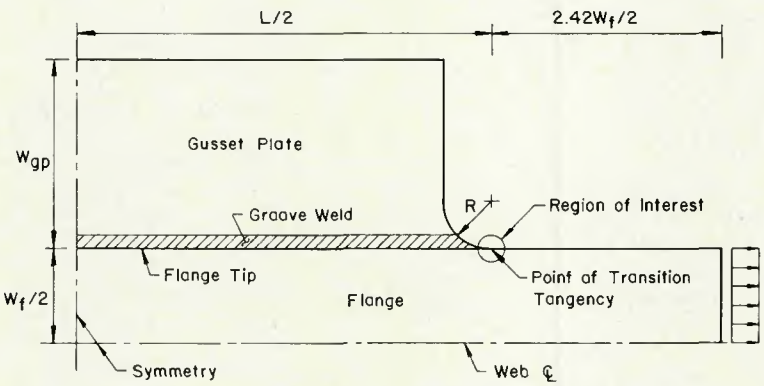

Fig. 1—Detail geometry for gusset plate investigation

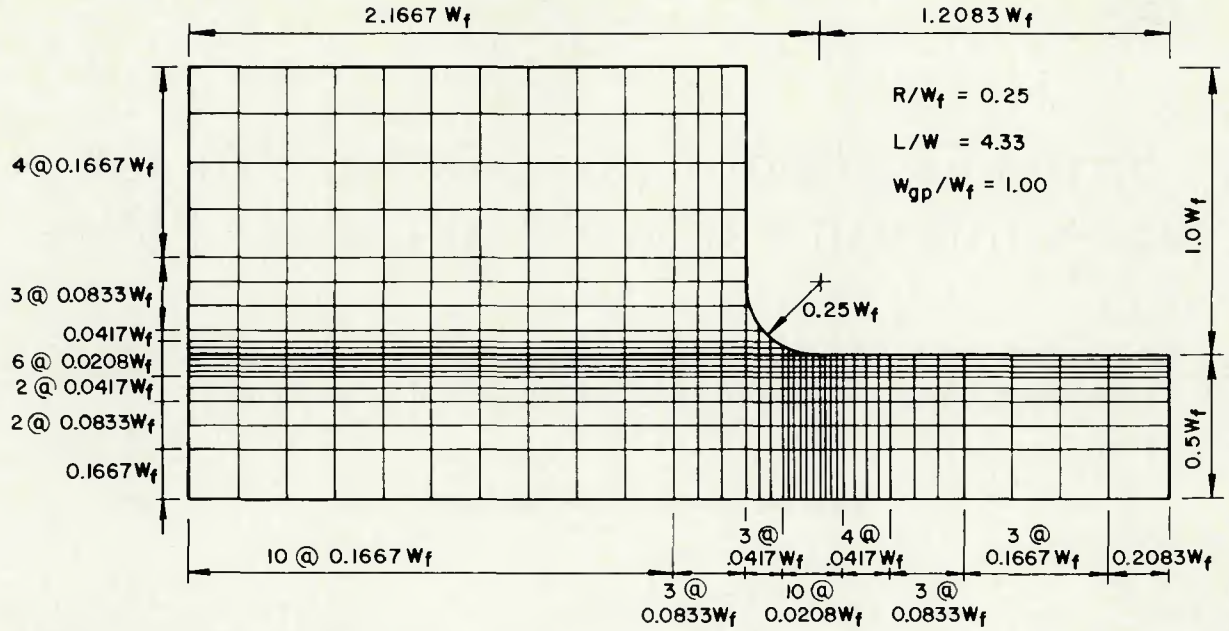

Fig. 2—Sample coarse mesh for gusset plate investigation

SCF. For gussets with small transition radii ($R/W_f < 0.5$), it was also necessary to employ a fine mesh which used the displacement output of the coarse mesh as input. SCF was derived from the maximum centroidal stress found in any of the fine elements.

A sample coarse mesh is given in Fig. 2. The boundary conditions prevent nodal displacements at and perpendicular to lines of symmetry—Fig. 1. In general, the flange discretization is unaffected by the various parametric changes—Table 1. In fact, the discretization of the gusset plate is also basically constant except the extent varies with the parametric values. Discretizations for other geometries can be developed by sketching the perimeter of the gusset on Fig. 2 and observing the mesh pattern within the boundaries. If extension of the width is required, the element sizes are identical to those in the current outer row. In the transition zone the mesh for a small radius is found by simply extending the given mesh lines.

The coarse mesh does contain some error due to the inaccurate representation of the circular transition with straight lines (chords) between nodes. The nodes themselves are positioned directly on the curve. One way to measure the geometrical error is by the largest deviation of any chord from the curve, as a percent of the radius.[2]

Figure 3 shows this error can be estimated from the chord length and the curve radius. The maximum chord length varies significantly from radius to radius since the larger radii reach the larger mesh sizes. However, the largest error is found for the smallest radius and is under 5%.

In the tangency region the error is always less than 1%. Such error in geometry is considered to have a negligible effect on results—particularly since the element's centroidal stress was used for SCF without extrapolation. Theoretically, singular stress conditions do exist at the skewed intersections of chords, but the angle difference between chords is always very slight and the intersections themselves receive no special finite element treatment.

The region of interest for highest stress concentration is in the vicinity of the point of transition tangency—Fig. 1. Based on photoelastic studies many references suggest that the maximum concentration occurs precisely at the point of tangency.[11,13,15,18] However, the findings of this study indicate the worst condition is slightly removed from this point. The deviation of the point of maximum concentration from the point of transition tangency could be caused by the chord approximation of the smooth curve.

In order to examine this premise, the results from two different coarse mesh discretizations were compared. One mesh size was equal to that in Fig. 2, while the other was twice as large in the region of interest. The resulting position of SCF from the point of tangency was found at roughly R/5 *for both discretizations.* (This approximation seems to be reasonable for any radius no matter what the gusset plate length, width, or thickness.) Hence,

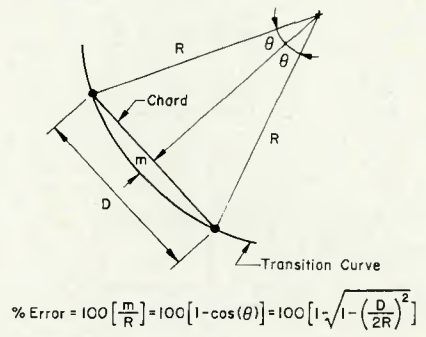

Fig. 3—Geometric error due to approximation of transition curve by chords

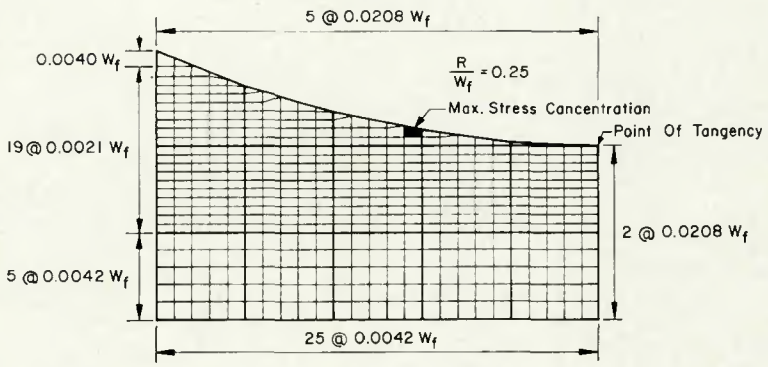

Fig. 4—Sample fine mesh for gusset plate investigation

the chord approximation did not appear to cause the shift in maximum concentration location.

The crack path can be assumed perpendicular to the flange tip or the direction of stress input.[5] Hence, SCF represents stress in the direction of applied stress, but not generally right at the point of tangency. Nevertheless, the nominal stress used to evaluate SCF was that which was input (i.e., that across the flange width prior to the transition).

Figure 4 presents a typical fine mesh discretization. Imposed boundary displacements are either taken directly or derived by linear interpolation from the output of the coarse mesh—Fig. 2. The mesh size is typical of fine discretizations for other radii. Since the maximum stress concentration factor is normally somewhat removed from the point of tangency, the fine mesh usually doesn't straddle that location. However, the cases of $R \leq 0.1\ W_t$ are exceptions to this rule.

Stress Concentration Results

The SCF value resulting from each combination of geometrical parameters is given in Table 1. The trend for each of the parameters is apparent from Figs. 5–8. SCF increases with increasing length, width, and thickness of gusset plate, but, as expected, SCF increases with decreasing transition radius.

Also plotted in Figs. 5–7 are curves derived by interpolation of Peterson's findings.[13] (No data are available in Peterson or elsewhere for varying thickness ratios—Fig. 8.) In all cases the results of this study have the same trend as those recorded by Peterson, but exceed them somewhat. The increase is generally on the order of 10%.

Regression analysis of values summarized in Table 1 yields the following SCF equation:

$$SCF = -1.115 \log\left(\frac{R}{W_t}\right) + 0.5370 \log\left(\frac{L}{W_t}\right) + 0.1384 \log\left(\frac{W_{gp}}{W_t}\right) + 0.2848\left(\frac{T_{gp}}{T_t}\right) + 0.6801 \quad (1)$$

The standard error of estimate s for eq (1) is 0.1322. This error is larger than that for stiffeners and cover plates[19] due to the additional variables involved.

The form of eq (1) permits a comparative rating of the importance of different variables. The coefficients indicate that radius R is more critical than length L, which is more critical than the width W_{gp}. The thickness ratio does not appear in the equation in logarithmic form so an exact comparison with other variables is not possible. However, from sample geometries the effect of thickness seems comparable to that of the length.

The stress concentration factor decay for the mesh geometry shown in Figs. 2 and 4 is plotted in Fig. 9. This curve exhibits the same pattern established by the stiffeners and cover plates.[19] Since SCF is lower the rate of decay is more gradual. The stress concentration factor reaches 1.0 at a distance of about 0.14 W_t. The actual distances vary with geometry although the general trend exhibited here is typical.

Table 1—Summary of Maximum Stress Concentration Factors for Gusset Plate Geometries

$\frac{R}{W_t}$	$\frac{L}{W_t}$	$\frac{W_{gp}}{W_t}$	$\frac{T_{gp}}{T_t}$	SCF
0.056	0.44	0.67	1.00	1.987
			0.50	1.496
	0.67		1.00	2.114
			0.50	1.803
	1.11		1.00	2.457
			0.50	2.245
	2.89	2.89	1.00	3.216
			0.50	2.787
0.083	0.67	1.00	1.00	2.022
			0.75	1.924
			0.50	1.770
			0.25	1.642
	1.00		1.00	2.277
			0.75	2.137
			0.50	1.922
			0.25	1.852
	1.67		1.00	2.554
			0.75	2.371
			0.50	2.163
			0.25	2.110
	4.33		1.00	2.737
			0.75	2.570
			0.50	2.519
			0.25	2.431
0.167	1.33	2.00	1.00	1.967
	2.00			2.101
	3.33			2.189
	8.67			2.229
0.250	1.00	1.00	1.00	1.658
			0.50	1.492
	1.67		1.00	1.790
			0.50	1.638
	4.33		1.00	1.870
			0.50	1.789
0.417	1.67	1.00	1.00	1.536
			0.50	1.392
	4.33		1.00	1.580
			0.50	1.425
		1.50	1.00	1.579
		0.50		1.562
0.500	1.67	1.00	1.00	1.440
			0.50	1.305
	2.33		1.00	1.461
	4.33			1.465
			0.50	1.386
1.000	4.33	1.00	1.00	1.254
			0.50	1.189
1.500	4.33	1.00	1.00	1.179
			0.50	1.117
2.000	4.33	1.00	1.00	1.132
			0.50	1.097

Stress Gradient Correction Factor

Correction Factor Results

The authors previously showed[19] that F_g can be isolated from other correction factors by using the Green's

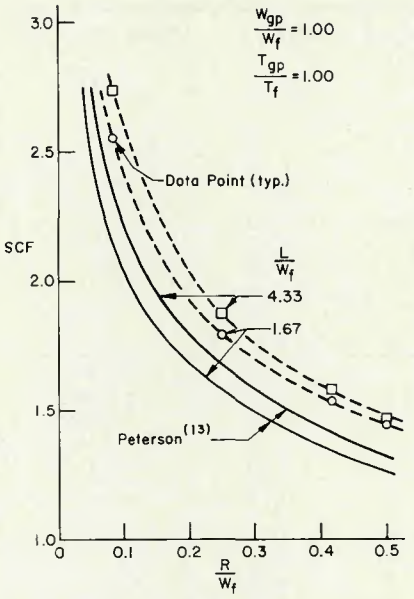

Fig. 5—Variation of maximum stress concentration factor with gusset plate transition radius

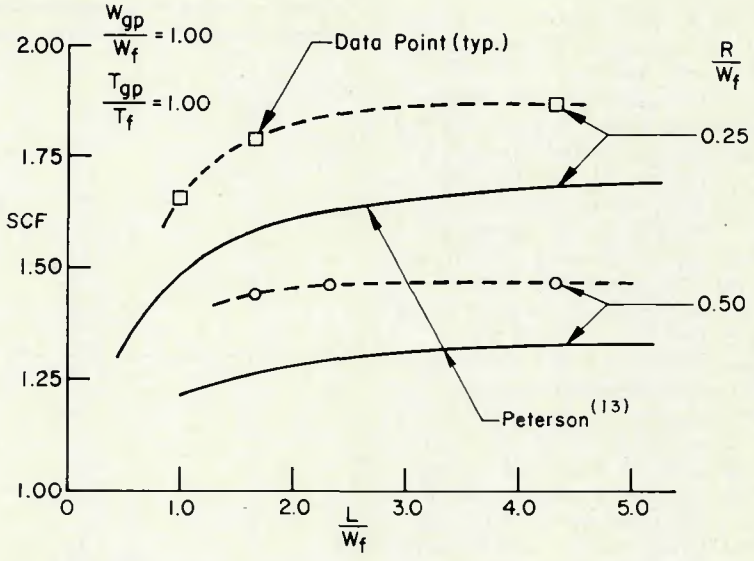

Fig. 6—Variation of maximum stress concentration factor with gusset plate length

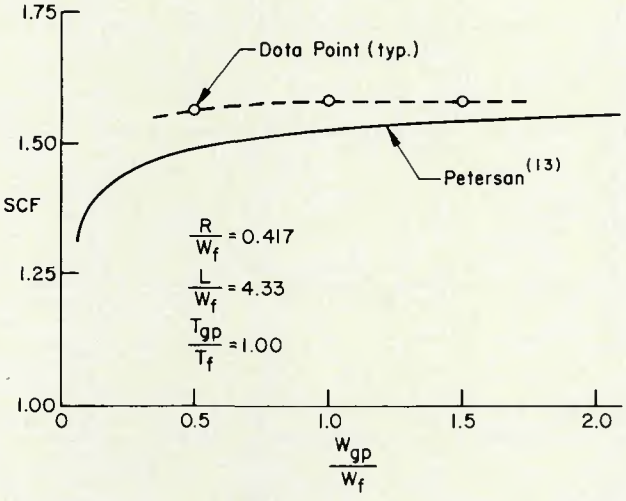

Fig. 7—Variation of maximum stress concentration factor with gusset plate width

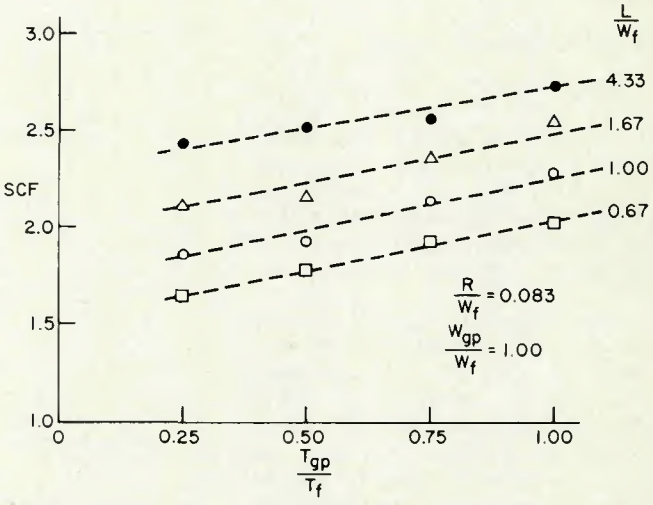

Fig. 8—Variation of maximum stress concentration factor with gusset plate thickness

function proposed by Albrecht and Yamada.[1] The numerical form of the F_g equation can be written as:

$$F_g = \frac{2}{\pi} \sum_{j=1}^{m} K_{tj} \left[\arcsin \left(\frac{l_{j+1}}{a} \right) - \arcsin \left(\frac{l_j}{a} \right) \right] \quad (2)$$

in which a is the crack length and l is the distance along the crack path. K_{tj} is the stress concentration in element j of the finite element discretization; l_{j+1} and l_j are the distances to opposite sides of element j. Limit m is the number of elements to crack length a.

Figure 10 presents F_g decay curves (F_g/SCF) for sample gusset plate details. As with the stiffeners and cover plates, SCF alone does not dictate the entire decay curve.[19] The F_g prediction process must account for a different mix of geometrical parameters than affects SCF alone.

Correction Factor Prediction

Analysts often desire a means of predicting F_g without finite element studies. One approximate formula for predicting F_g automatically is:[19]

$$\frac{F_g}{SCF} = \frac{1}{1 + \frac{1}{d}\alpha^q} \quad (3)$$

in which α is the nondimensionalized crack length, a/W_f. For a typical gusset plate geometry constants d and q can be taken as 1.158 and 0.6051, respectively.

A more precise procedure for predicting the entire F_g curve for arbitrary geometric conditions is comparable to that adopted earlier by the authors.[19] The actual F_g decay curves are correlated with the stress concentration decay from an elliptical hole in an infinite plate. Since SCF is generally less than 3.0, the hole is oriented with its minor semidiameter, h, perpendicular to the applied stress.

Figure 11a shows the ellipse shape is directly related to SCF. Knowing SCF [eq (1)], the proper ellipse shape can be established through rearrangement of the following equation:

$$SCF = 1 + 2\frac{h}{g} \quad (4)$$

Figure 11b demonstrates that the rapidity of stress concentration decay

Fig. 9—Stress concentration factor decay along prospective crack path across flange width at sample gusset plate detail

depends on actual hole size, not just SCF. Hence, to predict F_g from the elliptical hole K_t curve, semidiameter h must be known. For gusset plates the correlation between the curves is based upon equal life prediction for crack growth to the web line.

Stress concentration decay along the minor axis of an elliptical hole (uniaxial tension in major axis direction) can be expressed as:[4]

$$K_t = \left[\frac{1}{8} \left\{ 1 + 2e^{2\gamma} + e^{4\gamma} \right\} \left\{ 3 + 4e^{-2n} + e^{-4n} \right\} + \sinh(2n) \left\{ \cosh(2n) + \frac{1}{2}\cosh(2\gamma) + \frac{3}{2} \right\} \right] \Big/ \left(\cosh(2n) + 1 \right)^2 \quad (5)$$

in which n is the general elliptic coordinate and γ is the value of n associated with the hole perimeter. The elliptic coordinate can readily be evaluated.

$$\sinh(\gamma) = \left[\frac{1}{\left(\frac{g}{h} \right)^2 - 1} \right]^{1/2} \quad (6)$$

$$\sinh(n) = \left(1 + \frac{a}{h} \right) \sinh(\gamma) \quad (7)$$

For any given geometry and crack length, a, the stress concentration factor K_t is known if h is known. Further, if h has been correlated to equate K_t and F_g, then the stress gradient correction factor is also established.

A correlation study for the geometries in Table 1 has related the optimum ellipse size to the various geometrical parameters and initial crack size. The resulting regression curve is:

$$\frac{h}{W_f} = -0.01620 - 0.1105 \left(\frac{R}{W_f} \right) + 0.03307 \left(\frac{R}{W_f} \right)^2 +$$

(Equation continued on next page)

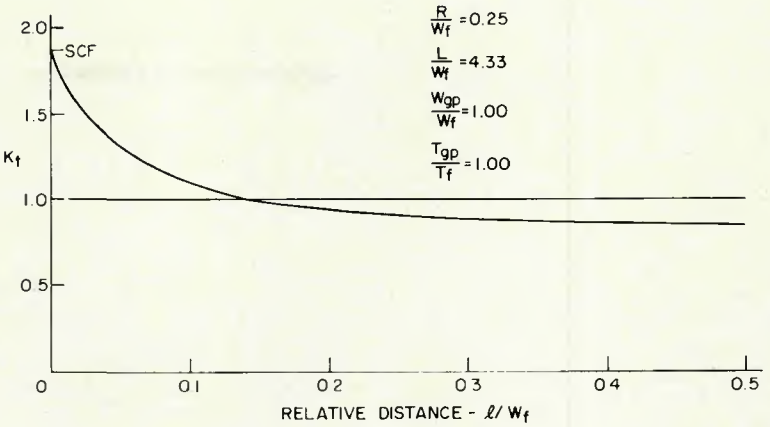

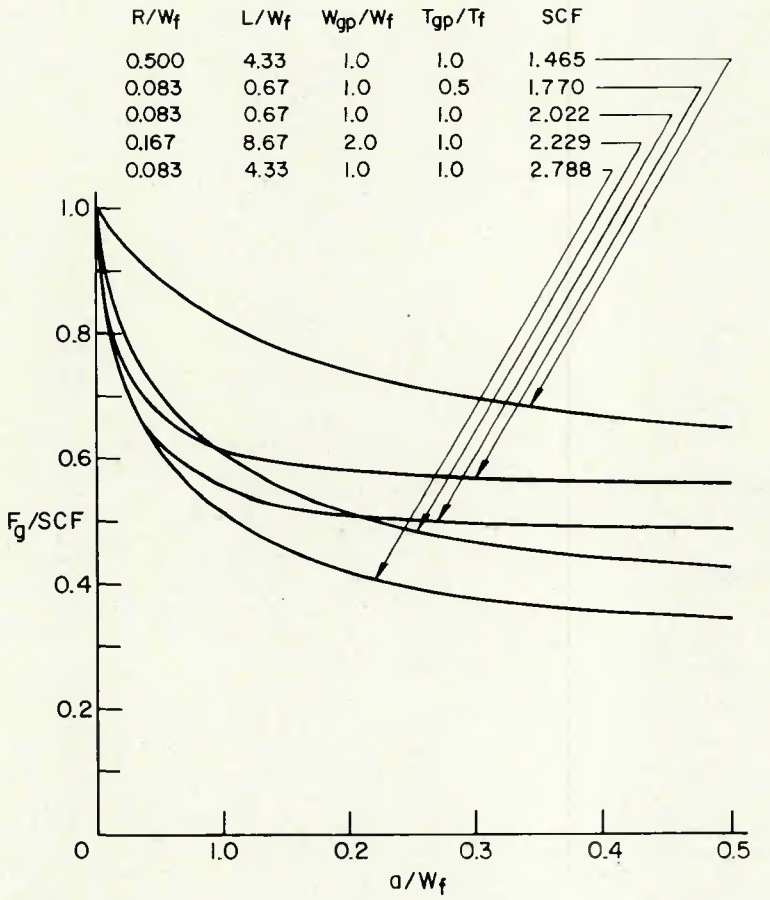

Fig. 10—F_g decay curves for sample gusset plate details

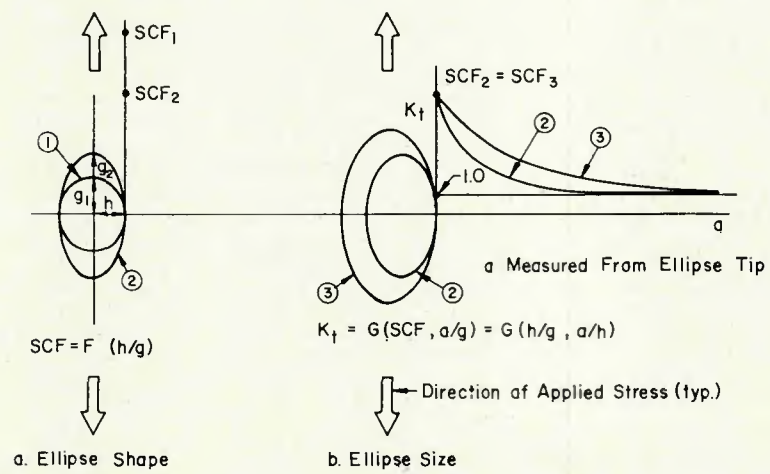

Fig. 11—Two steps required for ellipse correlation

(Equation continued from previous page)

$$0.02821 \left(\frac{L}{W_f}\right) - 0.002436 \left(\frac{L}{W_f}\right)^2 - 0.008776 \left(\frac{W_{gp}}{W_f}\right) + 0.004437 \left(\frac{W_{gp}}{W_f}\right)^2 + 0.08587 \left(\frac{T_{gp}}{T_f}\right) - 0.03291 \left(\frac{T_{gp}}{T_f}\right)^2 + 1.673 \left(\frac{a_i}{W_f}\right) - 43.49 \left(\frac{a_i}{W_f}\right)^2 \quad (8)$$

The standard error of estimate, s, for eq (8) is 0.01070.

The crack shape assumed in the above correlation study was quarter-elliptical (at the corner of the flange tip) until large enough to form a through (edge) crack.[5] Hence, the point of transition between quarter-ellipse and through crack was dictated by flange thickness. For thicknesses up to 1 in., h was found to be unaffected by crack shape considerations. However, larger thicknesses required a modification to eq (8).

For any flange thickness larger than 1 in., eq (8) should be multiplied by the following amplification factor:

$$1.0 + \frac{U}{34.54 \log \left(\frac{L}{W_f}\right)} \quad (9)$$

where $U = T_f - 1.0$ for $1 \text{ in.} < T_f \leq 2 \text{ in.}$

$= 1.0$ $T_f > 2 \text{ in.}$

Typically, this factor results in a change in h of less than 15%.

Conclusion

Stress concentration analyses have been conducted for various geometries of gusset plates groove-welded to flange tips. Each resulting stress concentration factor decay curve was transformed into a stress gradient correction factor for crack tip intensity through use of a Green's function. The correction factor curves were correlated with stress concentration factor decay from an elliptical hole in a uniaxially stressed plate. Each correlation resulted in an optimum size of elliptical hole for predicting the correction factor curve. Given the optimum ellipse size, automatic prediction of stress concentration effects on fatigue crack growth for arbitrary geometries is possible.

References

1. Albrecht, P., and Yamada, K., "Rapid Calculation of Stress Intensity Factors," *Journal of the Structural Division*, ASCE, Vol. 103, No. ST2, Proc. Paper 12742, February 1977, pp. 377-389.

2. Batcheler, R. P., "Stress Concentration at Gusset Plates with Curved Transitions," CE 103 Report, Lehigh University, Bethlehem, Pa., May 1975.

3. Bathe, K. J., Wilson, E. L., and Peterson, F. E., "SAP IV—A Structural Analysis Program for Static and Dynamic Response of Linear Systems," Earthquake Engineering Research Center Report No. EERC 73-11, University of California, Berkeley, California, June 1973 (revised April 1974).

4. Biezeno, C. B., and Grammel, R., "Elastic Problems of Single Machine Elements," Vol. II, *Engineering Dynamics*, Blackie & Son, Ltd., London, England, 1956, pp. 84-90.

5. Boyer, K. D., Fisher, J. W., Irwin, G. R., Roberts, R., Krishna, G. V., Morf, U., and Slockbower, R. E., "Fracture Analyses of Full Size Beams with Welded Lateral Attachments," Fritz Engineering Laboratory Report No. 399-2(76), Lehigh University, Bethlehem, Pa., April 1976.

6. Fisher, J. W., Albrecht, P. A., Yen, B. T., Klingerman, D. J., and McNamee, B. M., "Fatigue Strength of Steel Beams with Welded Stiffeners and Attachments," NCHRP Report No. 147, Transportation Research Board, National Research Council, Washington, D. C., 1974.

7. Gurney, T. R., *Fatigue of Welded Structures*, Cambridge University Press, London, England, 1968.

8. Kobayashi, A. S., "A Simple Procedure for Estimating Stress Intensity Factor in Region of High Stress Gradient," Significance of Defects in Welded Structures, Proceedings, 1973 Japan-U.S. Seminar, University of Tokyo Press, Tokyo, Japan, 1974, p. 127.

9. Lawrence, F. V., "Estimation of Fatigue-Crack Propagation Life in Butt Welds," *Welding Journal*, 52, (5), May 1973, Research Suppl., pp. 212-s to 220-s.

10. Maddox, S. J., "Assessing the Significance of Flaws in Welds Subject to Fatigue," *Welding Journal*, 53 (9), Sept., 1974, Research Suppl., pp. 401-s to 409-s.

11. Neuber, H., *Kerbspannungslehre*, 2nd edition, Springer-Verlag, Berlin, Germany, 1958, pp. 52-56.

12. Paris, P. C., and Sih, G. C., "Stress Analysis of Cracks," *Fracture Toughness Testing and Its Applications*, STP 381, American Society for Testing and Materials, Philadelphia, Pa., 1965, p. 30.

13. Peterson, R. E., *Stress Concentration Factors*, J. Wiley & Sons, New York, N. Y., 1974.

14. Randall, P. N., "Severity of Natural Flaws as Fracture Origins, and a Study of the Surface-Cracked Specimen," AFML-TR-66-204, August 1966 (published in ASTM STP 410, p. 88).

15. Seely, F. B., and Smith, J. O., *Advanced Mechanics of Materials*, 2nd edition, Wiley, New York/London/Sydney/Toronto, 1952.

16. Tada, H., Paris, P. C., and Irwin, G. R., *The Stress Analysis of Cracks Handbook*, Del Research Corporation, Hellertown, Pa., 1973.

17. Tada, H., and Irwin, G. R., "K-Value Analysis for Cracks in Bridge Structures," Fritz Engineering Laboratory Report No. 399.1, Lehigh University, Bethlehem, Pa., June 1975.

18. Timoshenko, S., *Strength of Materials, Part II—Advanced Theory and Problems*, 3rd edition, D. Van Nostrand, Princeton/New York/Toronto/London, 1956.

19. Zettlemoyer, N., and Fisher, J. W., "Stress Gradient Correction Factor for Stress Intensity at Welded Stiffeners and Cover Plates," *Welding Journal*, 56 (12), Dec. 1977, Research Suppl., pp. 393-s to 398-s.

Appendix

The following symbols are used in this paper:

- a = crack size
- D = chord length on gusset plate circular transition
- F_g = stress gradient correction factor
- g = major semidiameter of elliptical hole in an infinite plate
- h = minor semidiameter of elliptical hole in an infinite plate
- K_t = stress concentration factor
- ΔK = range of stress intensity factor
- *l* = distance along crack path from origin
- log = logarithm to base 10
- L = attachment length
- m = number of finite elements to crack length a; maximum distance between gusset plate circular transition and chord approximation
- R = radius of circular transition at end of groove-welded gusset plate
- s = standard error of estimate
- SCF = maximum stress concentration factor at the crack origin
- T_f = flange thickness
- T_{gp} = gusset plate thickness
- W_f = flange width
- W_{gp} = gusset plate width
- α = nondimensionalized crack length, a/W_f
- γ = value of elliptic coordinate *n* representing elliptical hole perimeter
- *n* = elliptic coordinate
- θ = half of angle delineating chord length of gusset plate circular transition